

ORIGINAL ARTICLE

Unique performance of thermal barrier coatings made of yttria-stabilized zirconia at extreme temperatures ($>1500^{\circ}\text{C}$)

Robert Vaßen^{1,2}  | Daniel Emil Mack¹  | Martin Tandler¹ | Yoo Jung Sohn¹  | Doris Sebold¹  | Olivier Guillon^{1,3} 

¹Forschungszentrum Jülich GmbH, Institute of Energy and Climate Research: Materials Synthesis and Processing (IEK-1), Jülich, Germany

²Institut für Werkstoffe, Ruhr-Universität Bochum, Bochum, Germany

³Jülich Aachen Research Alliance, JARA-Energy, Jülich, Germany

Correspondence

Robert Vaßen, Forschungszentrum Jülich GmbH, Institute of Energy and Climate Research: Materials Synthesis and Processing (IEK-1), Jülich, Germany.
Email: r.vassen@fz-juelich.de

Funding information

Deutsche Forschungsgemeinschaft; Helmholtz Association

Abstract

Yttria-stabilized zirconia (YSZ) has been for several decades the state of the art material for thermal barrier coating (TBC) applications in gas turbines. Although the material has unique properties, further efficiency improvement by increasing the temperature is limited due to its maximum temperature capability of about 1200°C . Above this temperature the deposited metastable tetragonal (t') phase undergoes a detrimental phase transformation as well as enhanced sintering. Both processes promote the failure of the coatings at elevated temperatures and this early failure has been frequently observed in gradient tests. In this paper, we now experimentally shown for the first time that under typical cycling conditions not the time at elevated temperatures leads to the reduced lifetime but the transient cooling rates. If cooling rates were reduced to 10K/s , TBC systems could be operated in a burner rig at a surface temperature well above 1500°C without showing a lifetime reduction. The explanation of these astonishing findings is given by the evaluation of energy release rate peaks during fast transient cooling in combination with the phase evolution during cooling with the used cooling rates.

KEYWORDS

thermal barrier coatings, thermal shock/thermal shock resistance, partially stabilized zirconia

1 | INTRODUCTION

For many decades thermal barrier coatings (TBCs) have been used to improve the efficiency of both aeronautical and stationary gas turbines.^{1,2} The most frequently used coating processes are electron beam physical vapor deposition (EB-PVD,³) and thermal spray processes such as atmospheric plasma spraying (APS,⁴). Due to the columnar, strain tolerant microstructure of the EB-PVD process, stress levels are reduced and the coatings are employed

for highly loaded parts of aero engines, especially the first row of the turbine blades. For stationary gas turbines and less loaded components of aero engines, thermal spray processes are the technology of choice. Considerable efforts were taken for the development of advanced TBC materials.⁴ However, the most frequently used material remains still for more than 40 years Yttria stabilized zirconia (YSZ), in which a stabilizer content of 7–8 wt% yttrium oxide is optimal.⁵ For both deposition processes, the YSZ is deposited in a so called t' phase which shows a high

This is an open access article under the terms of the Creative Commons Attribution License, which permits use, distribution and reproduction in any medium, provided the original work is properly cited.

© 2020 The Authors. *Journal of the American Ceramic Society* published by Wiley Periodicals LLC on behalf of American Ceramic Society (ACERS)

toughness and is generally accepted to have a good temperature capability up to about 1200°C.⁶ For a further improvement of the efficiency, higher operation temperatures are envisaged. However, it is known that at higher temperatures the metastable γ' phase undergoes a detrimental phase transformation and also accelerated sintering takes place. As both processes promote the failure of the coatings, 1200°C is accepted to be an upper temperature limit for long-term applications. Between the substrate, often a nickel base superalloy with excellent mechanical properties, and the ceramic topcoat TBC systems typically use an additional layer, the bond coat. The bond coat improves the bonding between topcoat and substrate. In addition, it protects the substrate from severe oxidation and corrosion as it forms a protective alumina scale (a thermally grown oxide—TGO) during oxidation as it is typically made of aluminum rich alloys such as aluminides or NiCoCrAlYs.⁷ Both the bond coat and the substrate will degrade fast at temperatures over 1200°C, so a test of a complete TBC system at elevated surface temperatures a thermal gradient is necessary. As thermal gradient tests are much more complex than isothermal tests in a furnace, often free-standing coatings are used to investigate the temperature capability of TBC materials and especially YSZ.^{8,9} In these investigations it was found that at elevated temperatures the non-equilibrium γ' phase basically decomposes into a mixture of an Y-lean tetragonal and an Y-rich cubic phase with several additional tetragonal phases appearing during the phase transformation.⁸ Upon cooling down to the ambient temperature, the tetragonal phase then transforms into the monoclinic phase. This phase transformation is accompanied by a rather large volume increase (about 4 vol.-%,¹⁰) which can lead to a disintegration of the coating.

Another detrimental process at elevated temperatures is sintering. All ceramic topcoats for TBC applications contain a large amount of porosity. This reduces the Young's modulus and as the strain is typically rather fixed given by the mismatch between substrate and topcoat, the stress level in the coatings is reduced. Reduced stress levels typically improve the lifetime of the coatings. The TBC elastic modulus increases as sintering progresses,^{11,12} resulting in larger magnitude of stored strain energy that may promote early failure and reduce lifetime.¹³ As discussed above, both described mechanisms are typically analyzed on free-standing coatings. An investigation of these effects in complete TBC systems with bond coat and substrate needs testing in a gradient. There are a rather large amount of rigs available (eg in Europe¹⁴), however often they are operated in an industrial environment and only limited experimental results are published. So the influence of especially very high surface temperatures on the lifetime of TBCs is hardly found in the literature.

A number of papers describe theoretically the influence of gradients on the lifetime of TBC systems.¹⁵⁻¹⁷ It is interesting

to note that from a purely elastic point of view, the gradient will reduce the stress level at room temperature after cooling down from a relaxed high temperature state as the mismatch strain is reduced. Hence, this would increase lifetime. Hutchinson et al¹⁶ considers the influence of gradients on the energy release rate for edge crack induced delamination for EB-PVD coatings mainly looking at the stationary case at high temperatures. This can lead to high energy release rates, however, a reduction is expected due to relaxation processes at elevated temperatures and furthermore, high temperature delamination is typically not observed experimentally.

Jackson et al¹⁸ also evaluated the transient phase in gradient testing. The authors can theoretically evaluate the energy release rates due to fast cooling in a gradient test. Due to the faster cooling of the ceramic topcoat in comparison to the metallic substrate, tensile stresses develop in the topcoat which can lead—depending on the cooling rates—to even higher energy release rates than in the fully cooled state. For rather high cooling rates well above 100K/s energy release rates of 50 J/m² can be expected for a 500 μ m thick TBC.¹⁸ These high energy release rates can explain the earlier failure of TBC systems tested at extremely high surface temperatures of above 1400°C. This reduction was recently observed¹⁹ and a corresponding explanation was given in terms of the energy release maximum during the transient cooling phase of the thermal cycling experiments. It was demonstrated in this investigation that the other degradation mechanisms often assumed to take place at elevated temperatures, namely sintering and monoclinic phase formation, are not of major importance.

The question now arises what happens if the cooling rate of the gradient test is reduced. Will the other degradation mechanisms such as sintering and phase transformation limit the lifetime of the TBCs? This question will be answered in the present paper.

2 | EXPERIMENTAL PROCEDURE

2.1 | Deposition of coatings

The substrates had a disk shaped geometry with a diameter of 30mm and a thickness of 3mm and were made from Inconel 738. The outer edge of the substrates was machined in a radius of curvature of 1.5 mm to reduce the stress level and avoid failure at sharp edges.

Before applying the topcoats, the disk shaped substrates were coated with a 150 μ m NiCoCrAlY (Oerlikon Metco, Amdry 386) bond coat by vacuum plasma spraying (VPS) in an Oerlikon Metco facility using a F4 plasma jet gun and 50 mbar booth pressure. The gun was operated at a power of 50 kW using a volumetric gas flow of 50 SLPM argon and

9 SLPM hydrogen as process gas at a stand-off distance of 275 mm.

A commercially available agglomerated and sintered 7YSZ Amperit powder (HC Starck Amperit 827.006, $d_{10} = 54 \mu\text{m}$, $d_{50} = 80 \mu\text{m}$, and $d_{90} = 112 \mu\text{m}$, 7.8 Mol-% $\text{YO}_{1.5}$ -stabilized ZrO_2) was used as feedstock powder for the ceramic topcoat. The investigated topcoats were deposited to a thickness of about 600 μm by atmospheric plasma spraying (APS) in a Multicoat facility (Oerlikon Metco, Wohlen, Switzerland) with a three-cathode TriplexProTM210 gun. The gun was operated with a power of 48 kW with 46 SLPM argon and 4 SLPM helium at a stand-off distance of 150 mm. Mercury porosimetry measurements were performed on free-standing coatings to avoid interaction with the substrate. These were produced by coating mild steel substrates with an intermediate NaCl layer with the YSZ topcoat and dissolving afterward the NaCl with water. The measurement gave a porosity of about 16%.

2.2 | Burner rig tests

The thermal cycling behavior of the coatings has been tested in a gradient test rig using a gas burner operating with natural gas/oxygen mixture.²⁰ The burner flame has about the diameter of the test samples and give a rather homogeneous temperature distribution with a slight temperature decrease towards the outer rim of the specimen. This temperature decrease is typically about 50K, but might increase with increasing surface temperatures. While heating the surface, the back side of the substrate was cooled by compressed air allowing the adjustment of the desired temperature gradient through the thermal barrier coating.

The surface temperature was measured with an infrared pyrometer KT15.99 IIP (Heitronics Infrarot Messtechnik GmbH, Wiesbaden, Germany) with a distance of roughly 60 cm between sample and pyrometer. For the monitoring of temperature a constant emissivity of the coatings was taken with the fixed value of 1. The emissivity value of 1 is an approximation, as more realistic values in case of YSZ TBCs are about 0.98²¹ in the wavelength range of the used pyrometer (9.6 μm -11.5 μm). For example, at object temperature of 1400°C the approximated value leads to an underestimation of the surface temperature which is below 30 K while the measurement uncertainty of the pyrometer itself is less than 11 K at this temperature. Emissions arising from the hot gas flame in the same spectral range lead to some increase of the pyrometer reading which, in part, counterbalance the effect of overestimated emissivity. As it appears difficult to precisely assess these competing effects, the same simplified approach was made for YSZ coatings expecting limited underestimation of the surface temperature.

A thermocouple mounted in a drilled hole to the center of the sample was used to measure the substrate temperature. Although the highest surface temperature of 1550°C was the focus of the present work, also 1400°C and 1500°C were used. The substrate temperature was kept constant at about 1050°C. As the thermal cyclic conditions slightly vary over time, the mean values were calculated from the logged temperature readings. These showed differences between the samples. With a 1-dimensional heat flux approximation ($q_{1D} = q_i = -k_i \cdot \Delta T_i / L_i$, with heat flux q , thermal conductivity k , temperature drop ΔT , and layer thickness L for each layer in i ="substrate", "bond coat", and "thermal barrier coating") and thermal conductivity values from literature (compiled in Ref. 22), the bond coat temperatures were found to be about 30 K to 40 K higher than the measured substrate temperatures. As the changes of thermal conductivity arising from microstructure evolution cannot be determined during testing, a fixed approximate value of 1 W/m/K was taken for the topcoats.

In standard tests, the burner heated for 5 minutes the sample and was then automatically moved away from the surface of the sample and an additional compressed air flow was applied to cool the surface during 2 minutes to achieve rapid cooling conditions. Controlled heating and cooling rates were achieved by continuous adaption of gas fluxes during transient phases. Cycling was stopped when a clearly visible spallation (about 20% of the surface area), or delamination of the coating occurred. For each surface temperature two samples were tested.

2.3 | Characterization

Metallographic cross sections have been prepared from the samples to investigate the microstructure and failure mode via Scanning Electron Microscopy (SEM) using a Zeiss Ultra 55 Field Emission Gun-SEM (Carl Zeiss Microscopy GmbH, Germany). The presented images are backscatter electron images, which were taken with an accelerating voltage of 8 kV. The TGO thickness was determined by measuring a number of 10 representative places of the TGO perpendicularly from the TGO/TBC to the TGO/BC interface. Places with strong internal oxidation and large oxide pegs were excluded. The TGO thickness was determined by measuring a number of 10 representative places of the pure TGO. At those 10 places a tangent line was laid on the top of the TGO and the thickness was measured perpendicularly from the point where the tangent touched the TGO, to the TGO/BC interface. Places with strong internal oxidation, large oxide pegs or areas with gaps and cracks within the TGO were avoided on purpose. Oxide pegs are often included by the digital imaging analysis programs which are not really connected to the TGO and/or yttria/hafnia rich precipitates close to the TGO are included

unintentionally. The thickness measurement was carried out using the measurement tools of the Zeiss SmartSEM software.

Further characterization of the coatings were also carried out using X-ray diffraction (Bruker-AXS/D4 Endeavor) for phase and crystallographic analysis and mercury intrusion porosimetry for pore size distribution (Pascal 140 and 440, Thermo Scientific, Hofheim, Germany). Rietveld analysis was performed using the TOPAS software V. 4.2 (Bruker AXS). It was carried out to identify the present phases qualitatively as well as quantitatively. The following references were chosen for a starting crystal structure model: tetragonal (Inorganic Crystal Structure Database, ICSD No. 86603), cubic (ICSD No. 75316), monoclinic (ICSD No. 60900). The peak profiles were refined using the fundamental parameters. The calculated lattice parameters enabled the assigning of the tetragonal YSZ into the t or t' -phases.

3 | RESULTS AND DISCUSSION

Typically in burner rig tests the burner is moved from the surface of the sample and then the surface is often cooled by compressed air. Even if the compressed air cooling is avoided, especially at highest surface temperatures, the initial cooling rate remains fast due to massive radiation cooling (a heat flow of 0.63 MW/m^2 can be expected for an emissivity 1 at 1550°C using Stefan-Boltzman's law). To avoid this effect, an experiment was performed in which the cooling rate was adjusted by a defined reduction of the burner heat flux with time. The established temperature profile obtained by this measure is shown in Figure 1 and compared to the conventional one. While for the conventional cycling an initial

cooling rate of about -100K/s is observed, this was reduced to about -10K/s in the modified cycle. It is assumed that the actual cooling rate is even higher but cannot be measured due to the limited time resolution of the pyrometer. An estimate of the mean cooling rate during the first 100ms can be estimated from Ref. 18 to be 2000K/s using the empirical cooling schedule given in the paper. An estimation according to Ref. 19 gives even higher value, in the first 10 ms the cooling rate is about $20\,000 \text{ K/s}$.

In addition, the heating rate is also slower in the new cycle and stationary gradient conditions are reached with slight delay. Despite this, the total time at high temperature is only slightly affected. In order to compensate the later arrival at low temperature the cooling phase was extended to 5 minutes.

The lifetime of the YSZ coating system in the burner rig testing for the different conditions is shown in Figure 2. Lifetime is here defined as the minimal cycle number at which 20% of the TBC coated area spalled-off. The results of the experiments with fast cooling rates are taken from a previous publication.¹⁹

Obviously, the low cooling rate leads to a huge improvement of the lifetime by a factor of more than 2. The lifetimes at a surface temperature of 1550°C with slow cooling seem to be even slightly higher than the one at a surface temperature of 1400°C with fast cooling. If a mean time per cycle at the highest temperature of about 4.5 minutes (see Figure 1) is taken, a total time at 1550°C of more than 100 hours (104 hours and 150 hours) results. Before these amazing results are further discussed, more details of the characterization will be presented.

The photos of the cycled samples are shown in Figure 3. All samples present a large delaminated area. The failure seems to run close to the interface topcoat and bond coat as

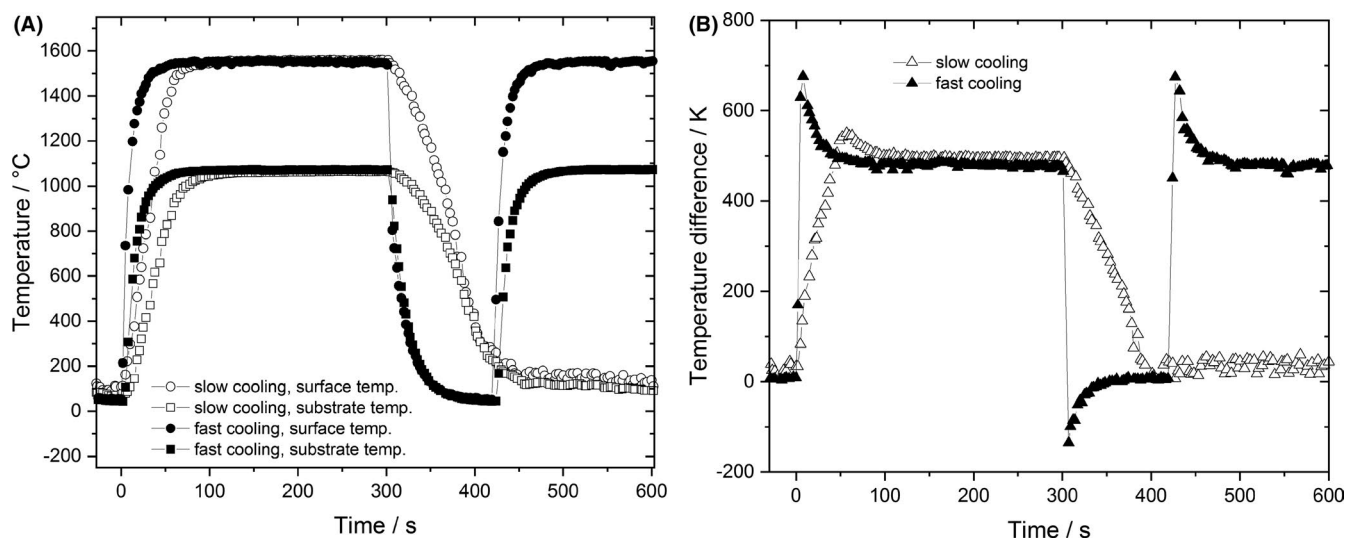


FIGURE 1 Temperature profiles during thermal cycles, filled symbols correspond to the standard thermal cycling (5 minutes heating, 2 minutes cooling), open symbols to the modified temperature profile (slow heating and cooling with 5 minutes heating, 5 minutes cooling). Circles show the surface, squares the substrate temperatures

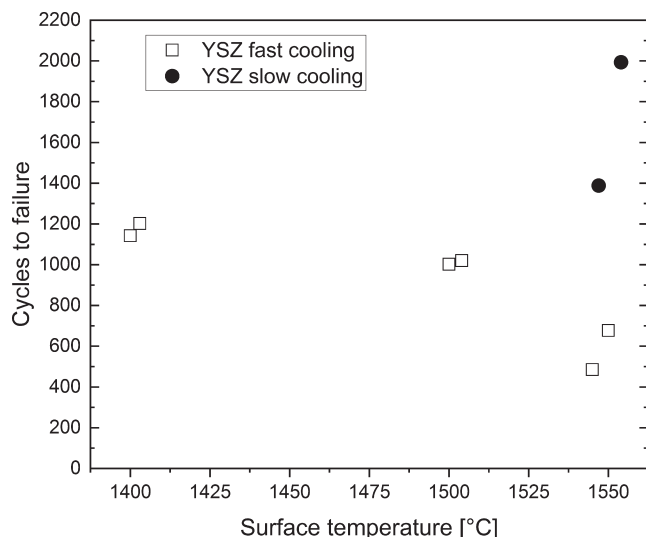


FIGURE 2 Number of cycles to failure for YSZ thermal barrier coatings as a function of the surface temperature using fast and slow cooling (s. Figure 1)

the oxidized bond coat is visible. Interesting is the roughening of the remaining TBC in the middle of the sample where the highest surface temperature is expected. At this location the samples also are more whitish. This is related to a thermo-mechanical degradation of the TBC triggered by different mechanisms. The authors assume that the extreme gradient close to the surface of the coatings lead to energy release rates high enough to promote layer wise spallation. The observed (see Figure 3) whitish color of the center of the samples after testing might be related to the extremely high temperatures reached when individual splats are only loosely bonded to the rest of the coating. These high temperatures can lead to a vaporization of impurities like Ca, which has a concentration of 330 ppm in the YSZ powder and can give a yellowish color of

the as-sprayed coatings.²³ The photos indicate that this type of degradation is less pronounced in the samples with the lower cooling and heating rates although the time at temperature was considerably longer. For a further evaluation metallographic cross sections of the cycled samples are evaluated (Figure 4). In the sample cycled with fast cooling and heating rates (see Figure 4A,B), a number of cracks are visible which corresponds to an ongoing damage of the coating material and which is also indicated in the central region of the samples in Figure 3. The higher magnification (Figure 4C) shows clearly the grown TGO at the bond coat/topcoat interface with a thickness of about 3 μm . Although the thickness is rather limited, the influence on the interfacial bonding which is determined by the critical energy release rate appears to be high enough, so that the critical one is equal to the apparent energy release rate. So a delamination occurs at the interface. Micrographs of a sample with reduced heating and cooling rate (Figure 4D-F) do not show a distinct difference of the microstructure of the coatings to the sample with the high cooling rate. The samples with slow cooling rates also show some longer cracks and reduced porosity levels in the regions close to the surface (Figure 4E). This indicates the closure of areas with small cracks and pores and the corresponding shrinkage will open the larger cracks. This demonstrates that sintering certainly took place. An indication of this sintering was found by indentation tests.¹⁹ However the coating is still rather intact showing only some crack formation even after more than 100 hours at 1550°C. Due to the long time at elevated temperature, the TGO also grew much thicker than for the high cooling rate sample, a value of about 6 μm could be determined.

As the operation temperatures during the here described tests have been extremely high, it is expected that a considerable phase segregation into cubic and tetragonal phase took

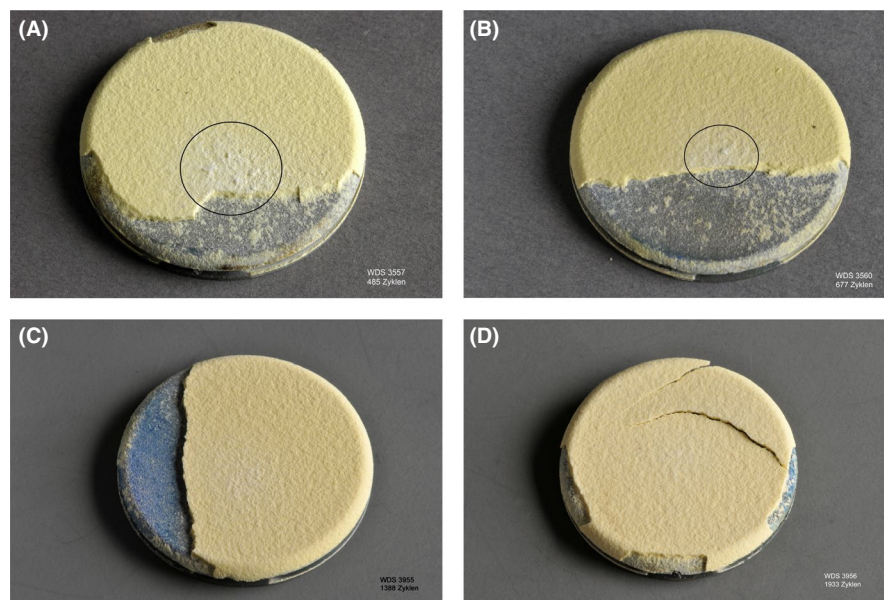


FIGURE 3 Photos of failed YSZ TBCs after cycling with a surface temperature of about 1550°C, top: fast heating and cooling, (A) 485 cycles and (B) 677 cycles, bottom: slow heating and cooling (C) 1388 cycles and (D) 1993 cycles. Circles indicate areas with visible damage [Color figure can be viewed at wileyonlinelibrary.com]

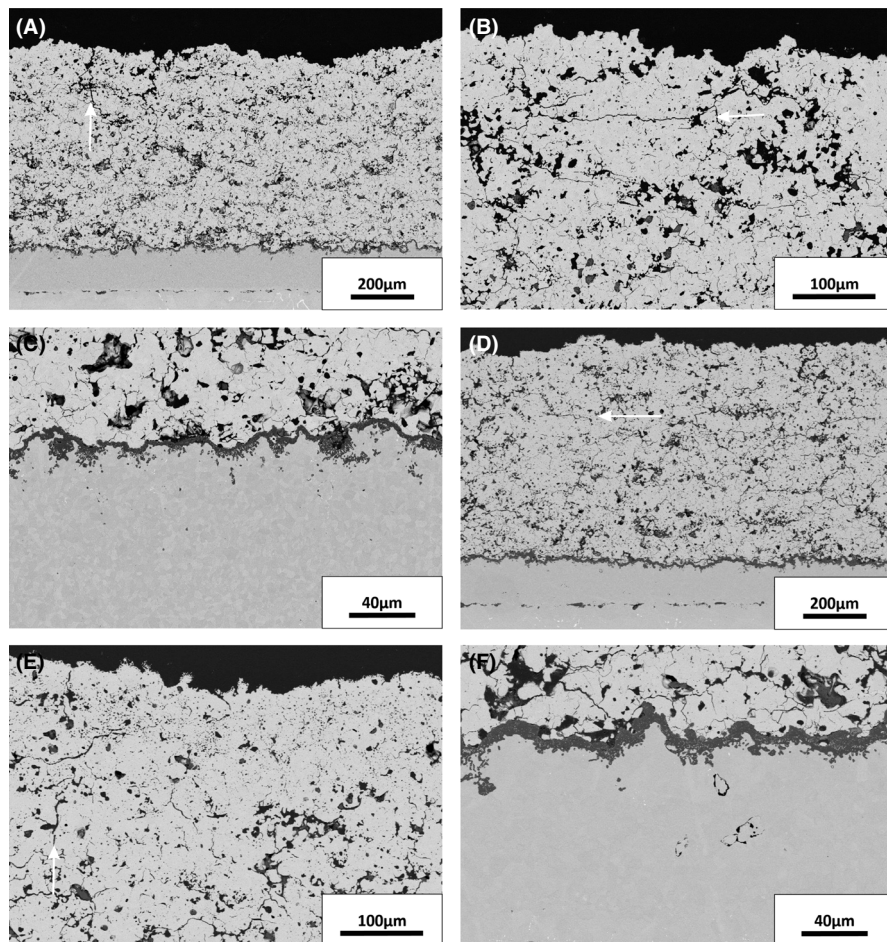


FIGURE 4 SEM micrographs of failed samples cycled with 1550°C surface temperature with fast heating and cooling rates (A, B, C, $T_{\text{surface}} = 1545^{\circ}\text{C}$, $T_{\text{bondcoat}} = 1079^{\circ}\text{C}$, cycles to failure 485) and slow rates (D, E, F, bottom, $T_{\text{surface}} = 1547^{\circ}\text{C}$, $T_{\text{bondcoat}} = 1086^{\circ}\text{C}$, cycles to failure 1388). Arrows indicate cracks

place with further monoclinic phase formation during cool down. In Figure 5, the results of Rietveld refinement data of XRD profiles of samples with fast and slow cooling are plotted as a function of the Hollomon–Jaffe parameter.²⁴ This approach combines temperature and time in a simple parameter HJP (similar to the Larson–Miller parameter):

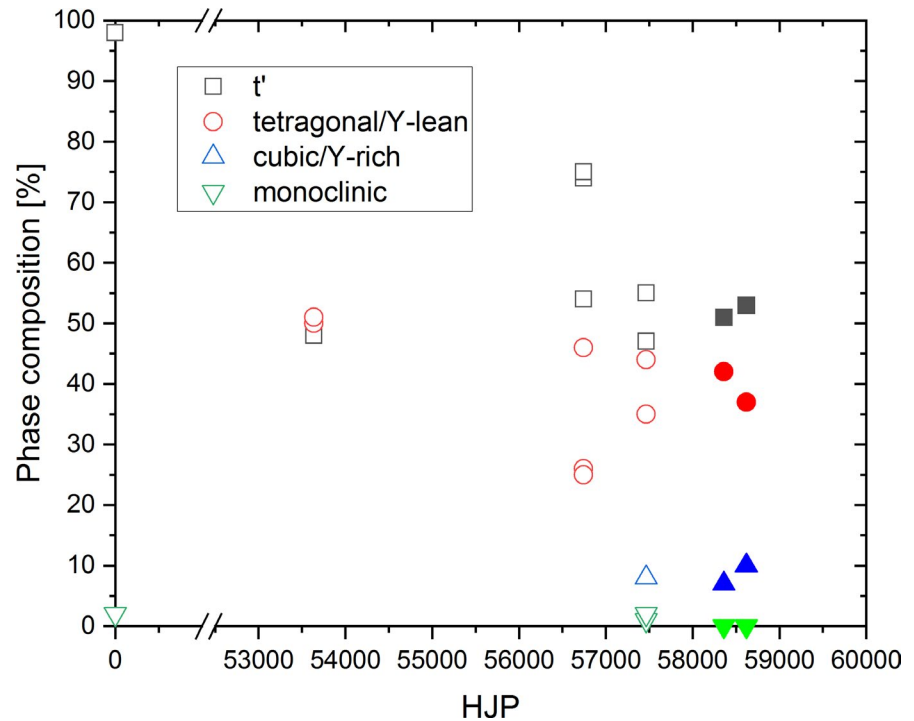
$$\text{HJP} = T(C + \ln t) \quad (1)$$

where T is the aging temperature in degrees Kelvin, t is the aging time in hours, and C is a constant for a given materials system. The HJP parameter was used in 25 to describe the phase evolution in free-standing YSZ thermal barrier coatings. The parameter $C = 27$ which is used here was determined in this analysis. The time t corresponds to the time at the highest temperature. In the present evaluation the amount of t' phase is within the experimental scatter rather constant with 50%. The Y-lean tetragonal phase lies round 40%. At the highest HJP values also about 10% of cubic phase (Y-rich) is observed. The amount of monoclinic phase is always in the low percentage range. This is in sharp contrast to the results shown in 25 where furnace tests with cooling rates of -10 K/min were performed.

Here at HJP numbers above 55 000 only Y-rich (cubic) and monoclinic phases are observed. These findings can be explained by a consideration of the oxygen vacancies in the coatings.

At higher temperatures, the amount of vacancies in equilibrium increase, stabilizing the tetragonal structure. If the cooling is performed quickly, the high equilibrium vacancy concentration is retained at room temperature and the afore-mentioned transformation is avoided. Slow cooling rates, on the contrary, reduce the vacancy concentration and increase the amount of monoclinic phases.²⁶ Slow cooling lead to 27% of monoclinic phase after a heat-treatment of 100 hours at 1500°C while less than 1% was observed after fast quenching.²⁶ Consequently, with respect to monoclinic phase formation fast cooling should reduce the transformation. As a conclusion the high amount of monoclinic phase is a result of the slower cooling rates down to room temperature in the furnace testing of the free-standing coatings which reduces the amount of vacancies stabilizing the tetragonal phase.²⁶ It should be mentioned here that the experiments in ²⁵ were performed on free-standing coatings. In the present work, full TBC systems including substrates were used. The substrate led to a compressive stress in the

FIGURE 5 Development of phase composition of the surface of the samples cycled in burner rigs as function of the Hollomon-Jaffe parameter (HJP). Open symbols correspond to high cooling rates, closed symbols to slow cooling rates [Color figure can be viewed at wileyonlinelibrary.com]



coating after cooling, this could reduce the amount of transformation into monoclinic phase. The experiments in ²⁶, which also have been performed on free-standing coatings, clearly demonstrated the effect of cooling rates. So it can be concluded that the transformation into the monoclinic phase can be avoided even without the presence of a substrate.

More interesting and new is the demonstration of the excellent thermo-mechanical performance of these coatings with the two tetragonal t' and t (Y-lean) phases, and some cubic phase (Figures 2 and 5). The most detrimental load is the extremely fast cooling at the beginning of the cool down phase. If this can be avoided by adjusting the cooling phase, the thermally aged material with tetragonal and some cubic phases can withstand the harsh thermal cycles. Indeed, the calculation of the energy release rate according to the approach given in ¹⁹ results in values of about 1 J/m^2 if a cooling rate of 10 K/s is assumed for the surface. This is by more than two orders of magnitude lower than the result obtained for fast cooling (123 J/m^2) and can explain the huge lifetime benefit under the specific cyclic conditions. That means if the energy release rate related to the transients is small, that is, slow cooling, the coating will fail when the energy release rate due to the mismatch stress during cooling exceeds the critical energy release rate. With higher surface temperature during cycling, the mismatch stress will be reduced and hence the energy release rate. This might be the reason why the lifetime at 1550°C is even slightly longer than that at 1400°C . It also should be mentioned that the topcoat in the vicinity of the interface topcoat bond coat, where the temperatures remain relatively low and cracks propagate in conventional

oxidation induced failure, is not affected by the high surface temperatures.

In the appendix, an approximate formula is derived which estimates the maximal energy release rate G_{\max} for a delamination crack at the interface:

$$G_{\max} \approx \frac{1}{6} (\alpha \Delta T)^2 E d \frac{\cdot T_c - \cdot T_{\text{sub}}}{\cdot T_c} \quad (2)$$

with α , E , and d being the thermal expansion coefficient, the Young's modulus, and the thickness of the coating, ΔT is the maximum temperature drop of the surface, and $\cdot T_c$, $\cdot T_{\text{sub}}$ the mean cooling rates of surface and substrate. For the here used TBC system with a maximum temperature drop of 1500 K a maximum value of 480 J/m^2 results. This value is much higher than typical critical energy release rates of TBCs systems and hence, even with smaller temperature drops the transient cooling can explain the failure of the TBC systems. As shown in the Appendix the substrate in the present case cools down with a rate of about 50 K/s , so that cooling should be faster than this value to have a considerable effect of the transient phase on the performance. If cooling is too fast, the heat front cannot diffuse fast enough through the whole coating. Such high cooling rates might lead to spallation of single splats or layers from the surface. A first indication of such a failure mechanism might be the crack parallel to the surface seen in Figure 4B. However, for cooling rates above about 1000 K/s no considerable further promoting effect for the spallation of the complete coating is expected.

The outlined explanations of the different failure modes are summarized in Figure 6. Of course, the details of the

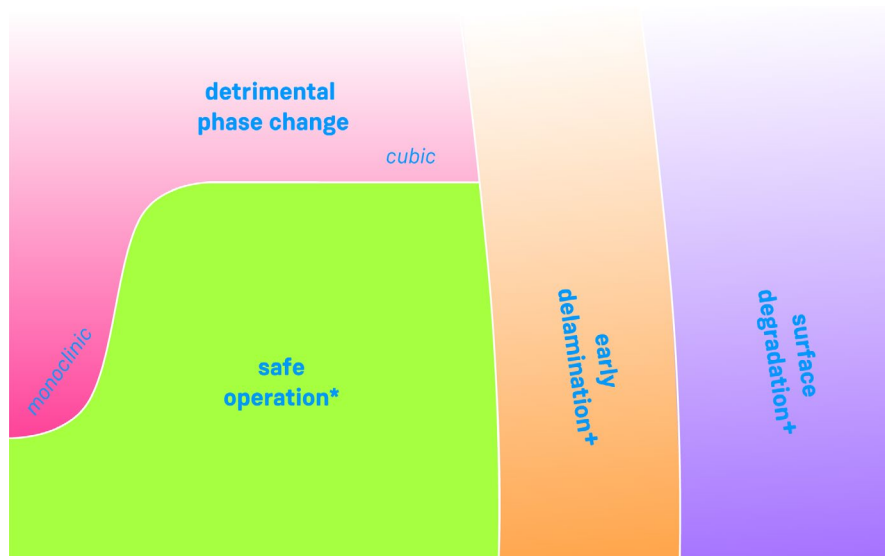


FIGURE 6 Failure maps of YSZ based TBC systems. * indicate failure by the oxidation of the bond coat, + indicate failure by the transients during fast cooling [Color figure can be viewed at wileyonlinelibrary.com]

given regimes will depend on the considered TBC system and have to be determined with more accuracy. Especially whether 1600°C is really the upper limit for safe operation needs to be confirmed. Nevertheless, the given failure map can provide a general insight in the failure of YSZ based topcoats at high surface temperatures and different cooling rates.

These findings can have a major impact on the gas turbine industry and the use of these coatings in service. The modification of the cooling cycle allows the use of the established YSZ based TBCs up to temperatures well above 1500°C. It only has to be guaranteed that the cooling rates are reduced to values below 100 K/s and that the cooling is maintained down to rather low temperatures of one hundred degree Celsius or slightly above. If that is not the case, a detrimental phase transformation into the monoclinic phase can occur. An option can be the use of reducing atmospheres to cool down to the lowest temperature. The low oxygen partial pressure can avoid the reduction of the number of oxygen vacancies, which stabilize the tetragonal structure. The up-take of oxygen will take place for oxygen contents above the equilibrium pressure which is with about 10^{-24} mbar at 1000°C low.²⁷ However, kinetic limitations can prevent sufficiently fast oxygen up-take.

The approach can be used especially for land-based turbines. It is advantageous if the engines are not operated at intermediate temperatures, which might be detrimental with respect to the formation of monoclinic phase. However, as long as the temperature is not below the tetragonal/monoclinic phase transformation line, the detrimental transition is avoided.²⁸ According to the YSZ phase diagram and the typical composition of YSZ TBC (about 8 Mol-% $\text{YO}_{1.5}$), even temperatures as low as 500°C can be tolerable.²⁸ A precise determination is difficult as the phase diagram is not published below 500°C. Nevertheless, for further cool down a short intermediate cycle to high

surface temperatures might be beneficial to establish again a high oxygen vacancy concentration. Then cooling down to room temperature should be done in a continuous process with intermediate cooling rates (eg 10 K/s). Also for stationary gas turbines, especially those which are operated with alternating loads (load flexible), and even for aero engines the proposed approach of reducing the initial cooling rate is advantageous as it reduces a major driving force for spallation of the topcoat. This general concept can also be advantageously adapted to new TBC systems based, for example, on pyrochlores as well as other protective coatings subjected to extreme temperature changes.

4 | SUMMARY

It was shown experimentally that fast cooling from elevated temperatures can be the origin of failure in thermal barrier coating systems. Fast cooling above 100K/s led to lifetime reduction by a factor of 2 to 3. If cooling rates were reduced to 10K/s, TBC systems could be operated in a burner rig at a surface temperature of about 1550°C without showing a lifetime reduction. With this defined cooling rate the peak in the energy release rates could be avoided. Furthermore, cooling down to low temperatures below 100°C with moderate cooling rates could additionally avoid tetragonal/monoclinic transformation and therefore lead to high lifetimes of the YSZ based coatings at extremely high surface temperatures.

From this outcome a stable, long-term operation of gas turbines using YSZ TBCs at surface temperatures above 1500°C is suggested by using defined modifications of the operation conditions.

ACKNOWLEDGMENTS

This work was supported by the Helmholtz Association. The authors thank Mr F. Kurze and Mr R. Laufs for

performing the plasma spraying experiments. In addition, the authors gratefully acknowledge the financial support of the German Research Foundation (DFG) through project no. VA 163/5-2.

DATA AVAILABILITY STATEMENT

The data supporting the findings of this study are available from the corresponding authors upon request.

ORCID

Robert Vaßen  <https://orcid.org/0000-0002-9198-3991>
 Daniel Emil Mack  <https://orcid.org/0000-0002-0365-4582>
 Yoo Jung Sohn  <https://orcid.org/0000-0002-7994-7269>
 Doris Sebold  <https://orcid.org/0000-0001-8595-8055>
 Olivier Guillon  <https://orcid.org/0000-0003-4831-5725>

REFERENCES

1. Vaßen R, Jarligo MO, Steinke T, Mack DE, Stöver D. Overview on advanced thermal barrier coatings. *Surf Coat Technol.* 2010;205(4):938–42.
2. Clarke DR, Oechsner M, Padture NP. Thermal-barrier coatings for more efficient gas-turbine engines. *MRS Bull.* 2012;37(10):891–8.
3. Schulz U, Saruhan B, Fritscher K, Leyens C. Review on advanced EB-PVD ceramic topcoats for TBC applications. *Int J Appl Ceram Tec.* 2004;1(4):302–15.
4. Bakan E, Vaßen R. Ceramic top coats of plasma-sprayed thermal barrier coatings: materials, processes, and properties. *J Therm Spray Technol.* 2017;26(6):992–1010.
5. Stecura S. Effects of compositional changes on the performance of a thermal barrier coating system. NASA TM-78976, National Aeronautics and Space Administration. 1978.
6. Darolia R. Thermal barrier coatings technology: critical review, progress update, remaining challenges and prospects. *Int Mater Rev.* 2013;58(6):315–48.
7. Naumenko D, Pillai R, Chyrkin A, Quadackers WJ. Overview on recent developments of bondcoats for plasma-sprayed thermal barrier coatings. *J Therm Spray Technol.* 2017;26(8):1743–57.
8. Krogstad JA, Krämer S, Lipkin DM, Johnson CA, Mitchell DRG, Cairney JM, et al. Phase stability of t'-zirconia-based thermal barrier coatings: mechanistic insights. *J Am Ceram Soc.* 2011;94:168–77.
9. Miller RA, Smialek JL, Garlick RG. Phase stability in plasma-sprayed partially stabilized zirconia-yttria. In: Heuer A.H., Hobbs L.W., editors. *Advances in Ceramics*. Columbus, OH: The American Ceramic Society, 1981; pp. 241–253.
10. Lange FF. Transformation toughening - Part 1 Size effects associated with the thermodynamics of constrained transformations. *J Mater Sci.* 1982;17(1):225–34.
11. Eaton HE, Novak RC. Sintering studies of plasma-sprayed zirconia. *Surf Coat Tech.* 1987;32(1–4):227–36.
12. Ahrens M, Vaßen R, Stöver D, Lampenscherf S. Sintering and creep processes in plasma-sprayed thermal barrier coatings. *J Therm Spray Technol.* 2004;13(3):432–42.
13. Vaßen R, Giesen S, Stöver D. Lifetime of plasma-sprayed thermal barrier coatings: comparison of numerical and experimental results. *J Therm Spray Technol.* 2009;18:835–45.
14. Vaßen R, Cernuschi F, Rizzi G, Scrivani A, Markocsan N, Östergren L, et al. Recent activities in the field of thermal barrier coatings including burner rig testing in the European Union. *Adv Eng Mater.* 2008;10:907–21.
15. Sundaram S, Lipkin DM, Johnson CA, Hutchinson JW. The influence of transient thermal gradients and substrate constraint on delamination of thermal barrier coatings. *J Appl Mech.* 2012;80(1):11002–13.
16. Hutchinson J, Evans A. On the delamination of thermal barrier coatings in a thermal gradient. *Surface Coat Technol.* 2002;149(2–3):179–84.
17. Öchsner M. Ein Beitrag zur Lebensdauervorhersage von keramischen Wärmedämmschichten. *Fortschritt-Berichte VDI Reihe 18 Nr. 263*, Düsseldorf, 2001.
18. Jackson RW, Begley MR. Critical cooling rates to avoid transient-driven cracking in thermal barrier coating (TBC) systems. *Int J Solids Struct.* 2014;51(6):1364–74.
19. Vaßen R, Bakan E, Mack D, Schwartz-Lückge S, Sebold D, Jung Sohn Y, et al. Performance of YSZ and Gd₂Zr₂O₇/YSZ double layer thermal barrier coatings in burner rig tests. *J Eur Ceram Soc.* 2020;40(2):480–90.
20. Traeger F, Vaßen R, Rauwald K-H, Stöver D. Thermal cycling setup for testing thermal barrier coatings. *Adv Eng Mater.* 2003;5:429–32.
21. Eldridge JJ, Spuckler CM, Street KW, Markham JR. Infrared radiative properties of yttria-stabilized zirconia thermal barrier coatings. *Ceram Eng Sci Proc.* 2002;23(4):417–30.
22. Vaßen R, Giesen S, Stöver D. Lifetime of plasma-sprayed thermal barrier coatings: comparison of numerical and experimental results. *J Therm Spray Technol.* 2009;18(5–6):835–45.
23. Paje SE, Llopis J. Photoluminescence-spectra study of yttria-stabilized zirconia. *Appl Phys A.* 1993;57(3):225–8.
24. Hollomon JH, Jaffe LD. Time-temperature relations in tempering steel. *Trans AIME, Iron Steel Div.* 1945;162:223–49.
25. Lipkin DM, Krogstad JA, Gao Y, Johnson CA, Nelson WA, Levi CG. Phase evolution upon aging of air-plasma sprayed t'-zirconia coatings: I - Synchrotron X-ray diffraction. *J Am Ceram Soc.* 2013;96(1):290–8.
26. Moon J, Choi H, Kim H, Lee C. The effects of heat treatment on the phase transformation behavior of plasma-sprayed stabilized ZrO₂ coatings. *Surf Coat Technol.* 2002;155(1):1–10.
27. Greenwood NN, Earnshaw A. *Chemistry of the Elements*, 2nd edn. Amsterdam, the Netherlands: Butterworth-Heinemann; 1997.
28. Fabrichnaya O, Aldinger F. Assessment of thermodynamic parameters in the system ZrO₂-Y₂O₃-Al₂O₃. *Zeitschrift für Metallkunde.* 2004;95(1):27–39.

SUPPORTING INFORMATION

Additional supporting information may be found online in the Supporting Information section.

How to cite this article: Vaßen R, Mack DE, Tandler M, Sohn YJ, Sebold D, Guillon O. Unique performance of thermal barrier coatings made of yttria-stabilized zirconia at extreme temperatures (>1500°C). *J Am Ceram Soc.* 2021;104:463–471. <https://doi.org/10.1111/jace.17452>